

*Earth and Planetary Science Letters*, 26 (1975) 253–262

© Elsevier Scientific Publishing Company, Amsterdam – Printed in The Netherlands

POROSITY DETERMINATIONS AND THE THERMAL CONDUCTIVITY OF ROCK FRAGMENTS  
WITH APPLICATION TO HEAT FLOW ON CYPRUS

PAUL MORGAN\*

*Geology Department, Imperial College, London (Great Britain)*

Received February 3, 1975

Revised version received April 9, 1975

A standard core analysis technique has been modified to estimate porosities from measurements on rock fragments. For the range of rocks tested, chip-determined fractional porosities were within  $\pm 0.025$  of the values measured on solid-core samples. This has enabled thermal conductivity measurements on rock fragments to be corrected for the effect of porosity, yielding agreement with conductivity determinations on solid core generally to better than  $\pm 10\%$ . The application of this is illustrated by the determination of heat flow in a 300-m borehole in western Cyprus (latitude  $34^{\circ}54'N$ , longitude  $32^{\circ}34'E$ , elevation 82 m). A decrease in temperature gradient with depth is almost completely compensated for by increasing thermal conductivity, and the best value for heat flow at this site is  $23 \pm 4 \text{ mW m}^{-2}$ .

## 1. Introduction

In most modern theories of the evolution of the Earth's crust, geothermal mechanisms play an important, if not fundamental role. During the past decade, therefore, many terrestrial heat-flow values have been determined by the product of the local crustal temperature gradient with the local rock thermal conductivity. Temperature measurements are generally made in boreholes that have been drilled for other purposes, but, with the exception of mineral exploration holes, core samples are often not available, so that the standard methods for determining thermal conductivities (steady-state divided-bar techniques) [1–4] cannot be used.

For many boreholes the only samples available are drill cuttings and Sass et al [5] have devised a technique to use these cuttings in conductivity determinations. The rock conductivity is deduced from a steady-state measurement of the thermal conductivity of a copper and plastic cell containing water and saturated rock fragments. A simple model is then used to estimate the conductivity of the water saturated aggregate

from the conductivity of the cell, its contents, and the dimensions and conductivities of the materials of the cell. It has been demonstrated that where the conductivities of the constituents do not contrast by more than one order of magnitude, the conductivity of a mixture can be represented by the weighted geometric mean of the conductivities of its components [6]. If  $K_w$  and  $\phi$  are the thermal conductivity and volume fraction of water in the cell respectively, and  $K_a$  is the determined conductivity of the cell contents, the weighted geometric mean conductivity of the solid components of the cell contents,  $K_r$ , is given by:

$$K_r = K_w (K_a / K_w)^{1/(1-\phi)} \quad (1)$$

Assuming the rock to be isotropic,  $K_r$  represents its conductivity if its natural porosity is zero and in this case  $K_r$  can be used as an estimate of the in-situ rock conductivity.

For porous isotropic rocks eq. 1 must be modified to account for the interstitial water present in the in situ rock. To calculate porous-rock conductivities,  $K_{pr}$  Sass et al. [5] derive the expression:

$$K_{pr} = K_w (K_a / K_w)^{(1-\phi_0)/(1-\phi)} \quad (2)$$

where  $\phi_0$  denotes the natural fraction porosity of the uncrushed rock. For some boreholes, particularly oil wells, much information is available concerning the

\* Present address: Department of Geological Sciences, Southern Methodist University, Dallas, Texas 75275, U.S.A.

sediment porosities. In a great many holes, however, no such data are available. In order to extend the chip-conductivity method therefore, it is necessary to either modify the techniques to determine porous-rock conductivities more directly, or to estimate the natural-rock porosities from measurements on the rock fragments.

An attempt was first made to measure porous-rock conductivities directly. The volume fraction of water in the cell is determined from the capacity of the cell, and the difference between the weights of the cell, first packed with dry rock fragments and then after saturation with water under a moderate vacuum. It was reasoned that if the rock chips were saturated and the excess water removed before packing into the cell, then the volume fraction of water then determined from the subsequent cell weights would only represent the water in the inter-chip spaces. The cell contents could then be considered as a mixture of water and saturated rock fragments, and the porous-rock conductivity determined directly using eq. 1.

This technique was attempted with several rock-fragment samples but no consistent results could be obtained, the main problems arising in the removal of the excess water from the chips. In order to overcome this difficulty, organic liquids immiscible with water were used in place of water in the mixture with the saturated rock fragments. Aniline, chloroform and castor oil were tested using the appropriate liquid thermal conductivity in place of  $K_w$  in eq. 1, but again the results were unrepeatable and inconsistent. The possibilities of estimating natural-rock porosities from measurements on the rock fragments were then investigated.

As no routine methods for the measurement of rock-chip porosities were known to the author, an attempt was made to adapt a core analysis technique for use with rock fragments. One of the instruments used in routine laboratory porosity determinations is the Kobe porosimeter, a single-cell Boyle's law apparatus, the performance of which has been described by Beeson [7]. Successful techniques have been developed to use this apparatus to determine rock-fragment porosities for thermal conductivity purposes.

The design and working principles of the Kobe porosimeter are briefly described below, followed by a discussion of the new techniques developed for handling chip samples. The success of the method is illus-

trated by a comparison of the results of porosity measurements on solid-core samples with rock fragments crushed from these cores; by a comparison of thermal conductivity measurements on solid samples with determinations on the corresponding chip samples; and finally by the determination of heat flow in a 300-m water exploration borehole in the west of the island of Cyprus.

## 2. The Kobe porosimeter

Fraction porosity,  $\phi_0$ , is calculated from measurements of the bulk volume,  $V_b$ , and grain volume,  $V_g$ , of the sample using the expression:

$$\phi_0 = (V_b - V_g)/V_b \quad (3)$$

The bulk volume is measured simply from the volume of mercury that the sample displaces at atmospheric pressure, assuming that none of the rock pores are entered by the mercury. The grain volume is determined by the volume of helium that the sample displaces, measured by a method involving the saturation of the sample with helium under pressure and an application of Boyle's law.

The version of the Kobe porosimeter used in this study is shown in Fig. 1. A mercury pump is used to inject mercury into the sample chamber, and measurement of the volume of mercury injected is made to a precision of 1 mm<sup>3</sup> using a vernier scale on the calibrated pump barrel. The mercury level can be accurately located at two levels, the top and bottom contacts. Gas pressure in the sample chamber can be equalized with atmospheric pressure through the outlet valve, and helium can be introduced using the gas-control valve. A two-way tap was added in series with the latter valve to allow the sample chamber to be evacuated, as discussed later. Gas pressure in the sample chamber is measured by a mercury pressure gauge connected to the mercury in the pump body. Measurements on solid-rock samples are made on cylindrical cores approximately 25 mm long and 25 mm in diameter.

Detailed experimental procedures for the use of porosimeters vary between different apparatuses [7,8] but the fundamental principles are the same and the basic stages in the use of a Kobe porosimeter are outlined in Fig. 2. The equation used to calculate the sam-



Fig. 1. Diagram

ple grain vol  
 $V_g = (v_e - v_i)$   
 (notation as  
 of Boyle's la  
 suming isoth  
 curate to cal  
 the mercury  
 troduces som  
 $P_c$ . It is also  
 measurement

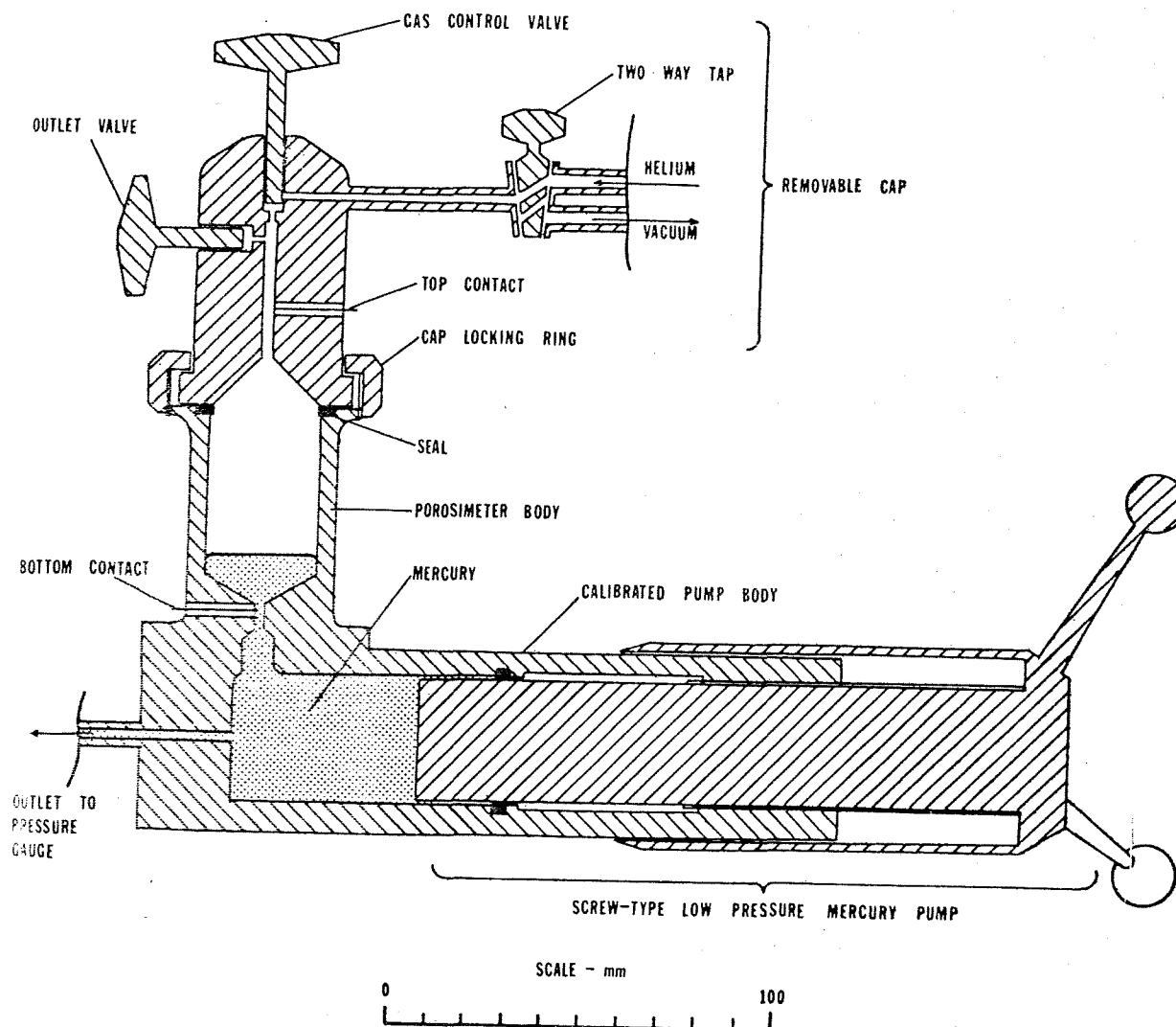


Fig. 1. Diagrammatic cross-section of the Kobe porosimeter.

ple grain volume:

$$V_g = (v_e - v_s)/(1 - P_a/P_c) \quad (4)$$

(notation as in Fig. 2) is derived from an application of Boyle's law to the gas in the sample chamber assuming isothermal conditions. In practice it is inaccurate to calculate  $V_g$  from eq. 4, as measurement of the mercury pressure and not the helium pressure introduces some uncertainties in the absolute value of  $P_c$ . It is also necessary at the start of each session of measurements to reject the first two or three deter-

minations as temperature differences through the apparatus introduce errors. Calibration runs are therefore made using a sample of known volume to determine a value for  $(1 - P_a/P_c)$ , and to ensure that the apparatus is in thermal equilibrium. A convenient method of effecting this is to pump a known volume of mercury,  $V_m$ , into the cell before the compression and again measure volume change,  $v_m$ , required to compress the helium to  $P_c$ . The measurement is repeated until consistent results are obtained, and used to calibrate the instrument by substituting the relevant

## BULK VOLUME DETERMINATION

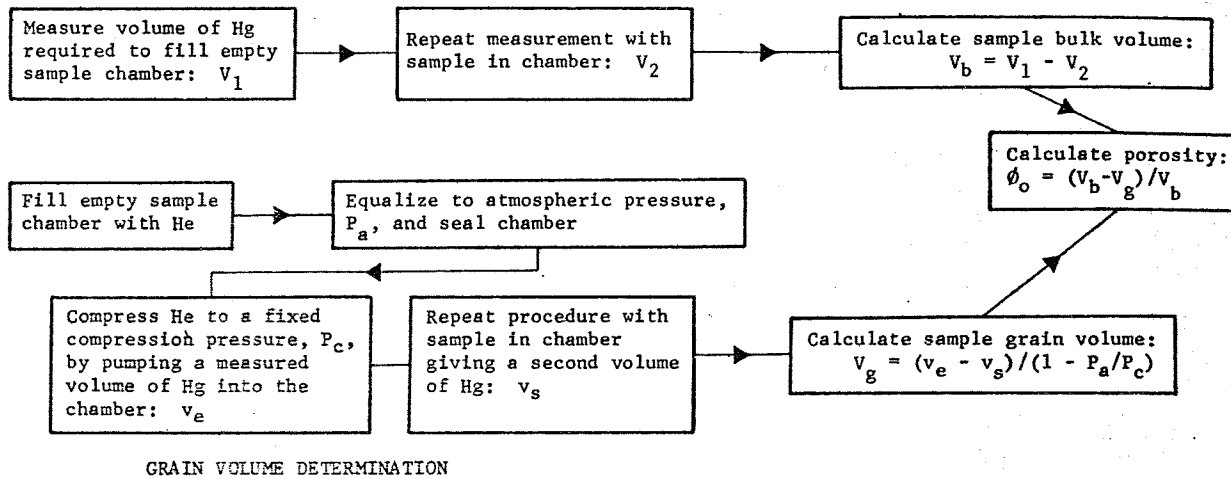


Fig. 2. Flow chart showing the basic stages in porosity determination using the Kobe porosimeter.

expression containing these values for  $(1 - P_a/P_c)$  in eq. 4, i.e.:

$$V_g = V_m(v_e - v_s)/(v_e - v_m) \quad (5)$$

Grain volumes are thereby calculated without the need for values of  $P_a$  and  $P_c$ , and before actual sample measurements are started the thermal equilibrium of the system is tested.

### 3. Porosity measurements on rock fragments

For porosity measurements on rock fragments, approximately  $12.5 \text{ cm}^3$  of the chips were loosely packed into a stainless steel cage (Fig. 3a). The bulk and grain volumes of the fragments are determined by subtracting the appropriate cage volume from the measured combined cage and chip volumes. Certain modifications to the basic techniques are necessary, however, to obtain consistent results.

In the bulk volume determinations it is important that the mercury completely surrounds all the chips and is not excluded from any regions by trapped pockets of air. To overcome this problem a two-way tap was fitted to the instrument, in series with the gas-control valve, to allow a moderate vacuum ( $0.7\text{--}1.4 \text{ kN m}^{-2}$ ) to be applied to the sample while the mercury is pumped into the cell. The system is then re-

turned to atmospheric pressure for the actual measurement. This has the undesired effect, however, of increasing the penetration of the mercury into the pores of the sample. By consideration of the pressure drop across a spherical mercury-air interface [9], it was estimated that, without the use of the vacuum

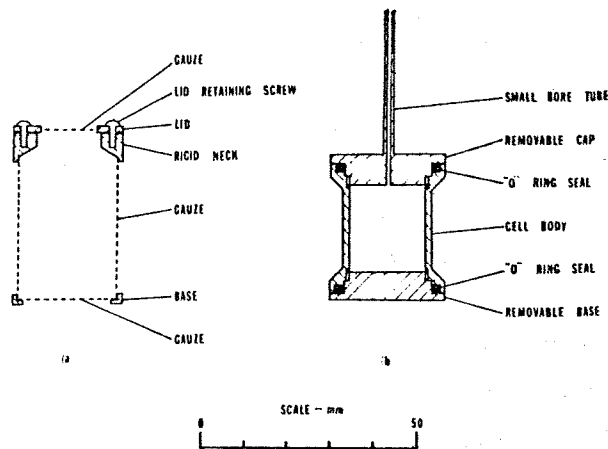


Fig. 3. a. Diagrammatic cross-section of porosity cage. The 26-mesh stainless-steel gauze is held into the stainless-steel body parts by epoxy resin. Horizontal cross-section circular. b. Diagrammatic cross-section of porosity cell. The cell was designed and constructed in stainless steel by the Exploration and Production Research Division of the British Petroleum Co. Ltd. Horizontal cross-section circular.

TABLE I

Porosities, bulk de

Sample description

Miocene sandy ma  
Altered dunite  
Agglomerate  
Miocene chalk  
Jurassic limestone  
Miocene sandy ch  
Basaltic pillow lav  
Basaltic pillow lav  
Miocene fine gra

and with a 15-m sample, mercury than 0.1 mm dia to reduce this th found to be sign cores listed in T obtain sensible r was also necessa the empty samp

In the grain-v to ensure that th um has access to stage in the com the chips, a spur will result. This pressure is used, mercury to be p solid-core sampl ( $18 \text{ lb./inch}^2$ ) ymal compression though reducing the apparatus. A ( $28 \text{ lb./inch}^2$ ) w porosities were calcu on chip samples the grain volume are compared w Table I and it ca ment to within error. All measu been made using

TABLE 1

Porosities, bulk densities and grain densities determined from measurements on solid-core and rock-chip samples. Densities in  $\text{Mg m}^{-3}$ 

Sample description	Fractional porosity			Bulk density		Grain density	
	chips	core	difference	chips	core	chips	core
Miocene sandy marl	0.111	0.089	-0.022	2.40	2.47	2.69	2.72
Altered dunite	0.023	0.007	-0.014	2.55	2.65	2.61	2.67
Agglomerate	0.109	0.115	+0.006	2.31	2.29	2.59	2.59
Miocene chalk	0.267	0.284	+0.017	1.96	1.89	2.67	2.64
Jurassic limestone	0.012	0.020	+0.008	2.68	2.63	2.71	2.68
Miocene sandy chalk	0.072	0.093	+0.021	2.50	2.40	2.70	2.65
Basaltic pillow lava	0.089	0.087	-0.002	2.54	2.49	2.79	2.73
Basaltic pillow lava	0.172	0.159	-0.013	2.13	2.17	2.57	2.58
Miocene fine grained sandstone	0.051	0.073	+0.022	2.51	2.46	2.65	2.65

and with a 15-mm head of mercury on top of the sample, mercury would penetrate openings larger than 0.1 mm diameter. The effect of the vacuum is to reduce this threshold to 0.006 mm. This was not found to be significant, however, in tests on the solid cores listed in Table 1, although it was found that to obtain sensible results with the use of the vacuum, it was also necessary to use the vacuum when determining the empty sample chamber volume.

In the grain-volume determinations it is necessary to ensure that throughout the compression, the helium has access to all the rock fragments. If at any early stage in the compression, the mercury isolates any of the chips, a spuriously high grain-volume determination will result. This effect is reduced if a relatively low compression is used, as this requires a smaller volume of mercury to be pumped into the chamber. Tests on solid-core samples using a compression of  $125 \text{ kN m}^{-2}$  ( $18 \text{ lb./inch}^2$ ) yielded results consistent with the normal compression of  $290 \text{ kN m}^{-2}$  ( $42 \text{ lb./inch}^2$ ), although reducing the sensitivity and repeatability of the apparatus. An intermediate value of  $190 \text{ kN m}^{-2}$  ( $28 \text{ lb./inch}^2$ ) was chosen for further tests. Grain densities were calculated from the results of measurements on chip samples crushed from solid cores by dividing the grain volumes by the sample weights. These results are compared with the solid-core determinations in Table 1 and it can be seen that the results are in agreement to within  $\pm 3\%$ , the estimated experimental error. All measurements in this study have therefore been made using a compression pressure of  $190 \text{ kN m}^{-2}$ .

Further checks on the chip grain volume determinations were made using a specially designed cell (Fig. 3b) to contain the rock fragments. This cell was packed with the chips (approximately  $4 \text{ cm}^3$ ) and the sample grain volume determined by measuring the combined cell and sample grain volume using the standard solid-core technique (Fig. 2) and subtracting the cell volume. The design of the cell allowed the normal compression of  $290 \text{ kN m}^{-2}$  to be used while preventing any mercury from coming in contact with the sample. Grain density results using this cell were found to agree with the results from the cage measurements to within the limits of experimental accuracy. Chip bulk volume measurements could also be made in this cell by removing the solid cell base, replacing it with a stainless steel gauze base, and using the porosity cage bulk volume technique described above. The porosity cage was preferred for these determinations, however, as it allowed a larger volume of sample to be used.

It is necessary to place a lower limit on the size of rock fragments used for porosity determinations as the porosity rapidly decreases as the chip sizes approach the grain size. All tests in this study were performed on fragments with diameters in the range 0.85 mm (20 mesh) to 2.0 mm as this range is representative of drill cuttings. The fact that core and chip determinations on the same samples agree implies that measurements on this size fraction provide estimates of whole-rock porosities.

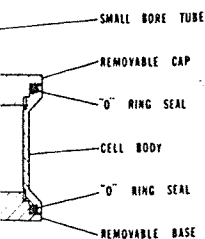
Final tests on the chip-porosity techniques have been made by comparing porosity determinations made

bulk volume:  
 $V_2$

calculate porosity:  
 $= (V_b - V_g) / V_b$

in volume:  
 $V_1 - P_a / P_c$

the actual measure-  
however, of  
mercury into the  
on of the pressure  
interface [9], it  
of the vacuum



porosity cage. The  
the stainless-steel  
cross-section circular.  
cell. The cell was  
by the Exploration  
British Petroleum Co.

on solid-core samples with measurements on rock fragments crushed from these cores. These results are shown in Table 1 and it can be seen that there is agreement to within  $\pm 0.025$ , which is within the experimental repeatability of the apparatus.

4. Application to thermal conductivity measurements

The effect of natural porosity on whole-rock thermal conductivities is demonstrated in Fig. 4. It can be seen that the reduction in conductivity is most marked for rocks with a high geometric mean conductivity of the solid constituents, but is still very significant even with relatively low-conductivity rocks. Porosity is therefore an important parameter in the determination of thermal conductivities from measurements on rock fragments using eq. 2.

Experimental studies have shown that rock fragment fractional porosities can be determined using modified techniques with the Kobe porosimeter to within  $\pm 0.025$ . The fractional error in the calculated conductivity,  $\partial K_{pr}/K_{pr}$ , due to an uncertainty  $\phi_0$  in po-

rosity, is given by:

$$\partial K_{pr}/K_{pr} = \phi_0 (\ln K_w - \ln K_r) \tag{6}$$

and the error limits for a  $\pm 0.025$  uncertainty in volume fraction porosity are shown in Fig. 3. It can be seen that this error is higher for more conductive rocks, rising from 3.0 to 5.7% as  $K_r$  increases from 2 to 6  $W m^{-1} C^{-1}$ . Sass et al. [5] give an accuracy limit of  $\pm 10\%$  for the basic chip conductivity measuring method, and this limit must be extended to  $\pm 16\%$  for higher-conductivity material where porosity measurements are included in the determination. If care is taken to remove all systematic errors from the measurements, however, it should be possible to improve this accuracy by repeating measurements on the same sample.

A comparison of conductivity determinations from solid-core and rock-fragment samples for most of the rock types listed in Table 1 is shown in Fig. 5 and tabulated in Table 2. Solid-core conductivities were measured in a brass divided-bar apparatus (as described by Beck [3] but with no guard-ring fitted to the bar), and chip conductivities were determined using

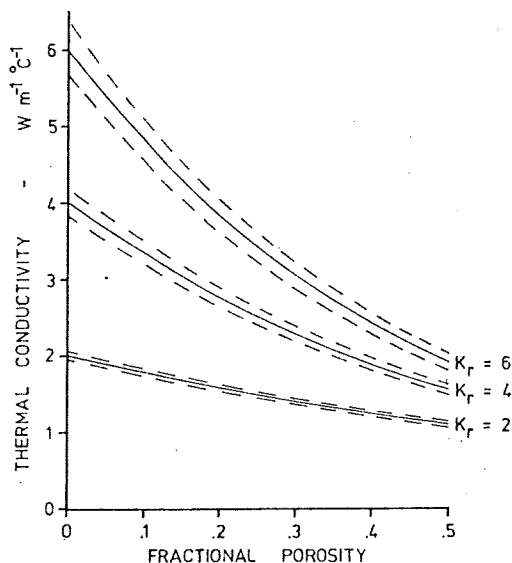


Fig. 4. The effect of porosity on thermal conductivity for different values of  $K_r$ . Dashed curves show the conductivity errors for a  $\pm 0.025$  error in fractional porosity.

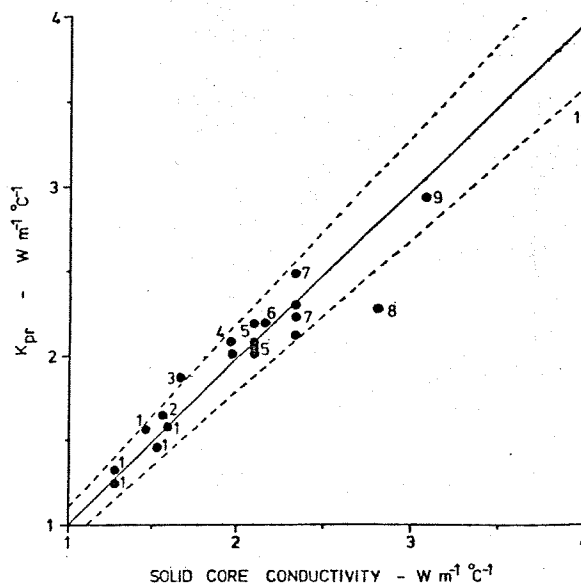


Fig. 5. Comparison between solid- and chip-determined conductivities. Dotted lines show the  $\pm 10\%$  error limit for  $K_{pr}$ . Numbers by points refer to sample lithology as listed in Table 2.

TABLE  
Conduct  
chip, po  
 $W m^{-1} C^{-1}$

Key S:  
no. ti

1 Ba  
la:

2 Ba  
3 M

4 M  
ch

5 M  
Pl

M  
gr  
st

6 M  
7 M  
Pl  
m

8 A  
9 M  
st

Where th  
determin  
tions is gi  
mined by

the same  
porosity as  
crushed  
conduct  
due to c  
and chip  
limit for  
terminat  
the pred  
results a  
the high-  
difficult



TABLE 2

Conductivity data used in Fig. 5;  $K_r$ ,  $K_{pr}$ ,  $K_d$ : Non-porous chip, porous-chip and solid-core conductivities respectively in  $W m^{-1} ^\circ C^{-1}$

Key no.	Sample description	$K_r$	$\phi_0$	$K_{pr}$	$K_d$	Dif
1	Basaltic pillow lava	1.34	0.101	1.24	1.28	-3.3
		1.47	0.124	1.31	1.28	+1.6
		1.82	0.150	1.56	1.46	+6.9
		1.86	0.216	1.46	1.53	-4.7
		1.93	0.172	1.58	1.59	-0.8
		4.03	0.089	3.41	3.98	-14.5
		1.96	0.146	1.65	1.56	+6.2
2	Basalt	2.80	0.267	1.87	1.67	+12.1
3	Miocene chalk	3.37	0.302	2.01	1.97	+1.9
4	Miocene sandy chalk	2.29	0.072	2.08	1.96	+6.2
5	Miocene to Pliocene marl	2.32	0.105	2.01	2.09	-3.6
		2.62	0.164	2.05	2.09	-1.0
		2.52	0.136	2.08	2.09	-0.4
		2.56	0.109	2.19	2.09	+5.2
	Miocene fine grained sandstone	2.24	0.051	2.10	2.12	-1.2
6	Miocene marl	2.71	0.143	2.19	2.15	+1.6
7	Miocene and Pliocene sandy marl	2.48	0.111	2.12	2.33	-9.1
		2.69	0.127	2.23	2.33	-4.5
		2.60	0.095	2.30	2.33	-1.4
		2.93	0.151	2.31	2.33	-1.1
		3.04	0.132	2.48	2.33	+6.3
8	Altered dunite	2.35	0.023	2.28	2.80	-18.5
9	Mesozoic limestone	3.04	0.025	2.92	3.05	-4.2

Where the samples were very friable making single solid-core determinations unreliable, the mean of the solid determinations is given.  $\phi_0$ : Fractional porosity. Dif: Differences determined by  $Dif = (K_{pr} - K_d)/K_d \cdot 100$ .

the same apparatus [5], corrected for the effect of porosity as described above. The chip samples were crushed from the actual cores on which the solid-core conductivities were measured to minimize variations due to compositional heterogeneity. Most of the solid and chip conductivities agree to within the  $\pm 10\%$  error limit for  $K_{pr}$  and, as the precision of a single solid determination was generally  $\pm 3\%$ , these are well within the predicted limits of experimental error. Only two results are significantly outside the  $\pm 10\%$  error limit: the high-conductivity basaltic pillow-lava chips were difficult to permeate with helium during the grain-

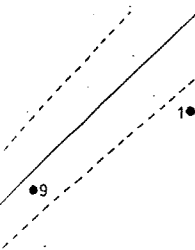
volume measurement, and the porosity determination is thought unreliable; the altered dunite rock fragments were possibly hydrated during saturation for the conductivity measurement, as slight swelling occurred and some of the sample was lost from the conductivity cell, making the conductivity determination inaccurate. The results then show the success of the incorporation of the porosity measurements into the chip conductivity technique.

Horai and Simmons [10] have adopted an alternate technique for measuring the thermal conductivity of rock fragments. The chips are crushed into powder, saturated with water, and the conductivity of the resulting mixture is measured by the needle-probe method [11]. As with the steady-state technique of Sass et al. [5], however, some estimate of the rock porosity is required to calculate the porous-rock conductivity. Determinations of porosities using the Kobe porosimeter as outlined above would allow this calculation to be made. King and Simmons [12] determined porosities for this purpose from density measurements on dry and water-saturated specimens of the uncrushed rock. As the size of the rock fragments decreases, however, this method of porosity determination becomes impractical as it becomes increasingly difficult to remove the excess water from the saturated chips. The Kobe porosimeter technique does not suffer from this problem and is therefore more generally applicable than the wet- and dry-density method.

Choice of the relationship for determining the thermal conductivity of the solid component of the fluid-solid mixture is made purely on an empirical basis. Sass et al. [5] have chosen the weighted geometric mean relationship (eq. 1) which has been adopted for the present study. With the needle-probe method both the geometric mean (e.g. see [12]), and the average of the upper and lower bounds given by Maxwell's relations for non-interacting spheres of one conductivity in a matrix of another (e.g. see [10,13]) have been used. The precision of the experimental data is not sufficiently high to indicate the more representative of these relationships. In a study of the thermal conductivity of vesicular basalt, Robertson and Peck [14] have concluded that the thermal conductivity of the fluid-solid rock system is best represented by a mean of parallel and series models or a quadratic relationship. Whichever relationship is chosen, however, the measurement of natural-rock porosities using the Kobe

(6)

uncertainty in volume  
3. It can be seen  
conductive rocks,  
decreases from 2 to 6 W  
accuracy limit of  
ity measuring meth-  
ed to  $\pm 16\%$  for  
e porosity measure-  
ation. If care is  
ors from the mea-  
ossible to improve  
ements on the same  
eterminations from  
les for most of the  
wn in Fig. 5 and  
conductivities were  
paratus (as de-  
ward-ring fitted to  
ere determined using



ip-determined con-  
error limit for  $K_{pr}$   
ogy as listed in

porosimeter will increase the precision of determinations of porous-rock conductivities.

### 5. Heat flow in Cyprus

The application of rock-fragment porosity determinations to terrestrial heat-flow determinations is demonstrated by the results from a 300-m water exploration borehole on Cyprus. The borehole penetrated Miocene marls, chalks, chert and gypsum of the Pakhna formation, but no solid-core samples were recovered. Drill cutting samples were collected, however, and the rock conductivities were estimated from measurements on these samples by the techniques outlined above. Measured porosities were in the range 0.18–0.47, and the effects of these on the calculated conductivities are shown in Fig. 6. Least-squares temperature gradients were calculated from the temperature data within each depth range represented by a conductivity sample and Fig. 6 shows some inverse correlation between the gradient and conductivity data. Component heat flow values were calculated using conductivity values both

corrected and uncorrected for porosity. It can be seen that there is less scatter in the former results.

Except for the upper 40 m of the hole, temperature logs made on 10 June 1970 and 14 May 1971 agreed to within  $\pm 0.02$  °C and the data are considered to be free from the effects of short-term transient disturbances. The heat flow for the interval 38–304 m was calculated to be  $19.4 \pm 0.1$  mW m<sup>-2</sup> using a least-square fit to the temperature and thermal resistance data [15]. Correction for the steady-state influence of local topography [16] increases this value to 21.0 mW m<sup>-2</sup> and corrections for the topographic evolution of the area increase this by a further 5–10% (based on data from Henson et al. [17] and Vaumas [18]). These corrections cannot explain the decrease in heat flow with depth shown in Fig. 6 and this could be the result of Quaternary climatic changes, horizontal variations in thermal conductivity, or regional water flow. Lack of information prevents the reliable estimation of these effects, and the best value for the heat flow is estimated to be  $23 \pm 4$  mW m<sup>-2</sup>.

Additional heat-flow data from Cyprus confirm this result [8], and marine heat-flow determinations

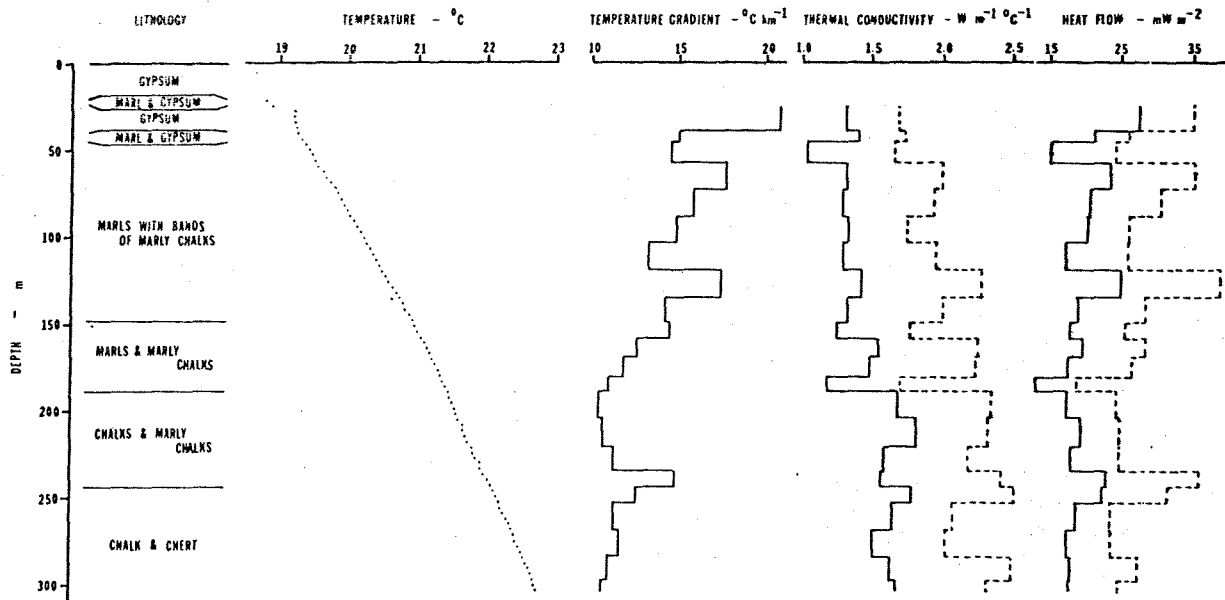


Fig. 6. Heat-flow results from Cyprus government water borehole PB35 (latitude 34°50'N, longitude 32°34'E, elevation 82 m). Drilling started 7 October 1969, completed 25 November 1969. Temperature logs made 10 June 1970 and 14 May 1971. Dashed lines show conductivities and calculated heat-flow values uncorrected for the effect of porosity.



in the eastern Mediterranean have yielded similar low values [19,20]. Discussions of these results are given by Erickson [19], Ryan et al. [20] and Morgan [8].

## 6. Conclusions

The results shown in Table I indicate that with a modification of the basic techniques the Kobe porosimeter can be used to estimate natural-rock porosities from measurements on rock fragments. Fractional porosities have been determined to within  $\pm 0.025$  which is quite adequate for the correction of thermal-conductivity measurements on chip samples for the effects of natural-rock porosity. Porous isotropic rock thermal conductivities determined from measurements on rock fragments agree to within  $\pm 10\%$  of solid-core determinations (Fig. 5). Random errors of this magnitude are acceptable for terrestrial heat-flow determinations, as variations in conductivity due to heterogeneity between hand samples are of the same order [5]. Data from a Cyprus borehole (Fig. 6) illustrate the application of the chip porosity and conductivity technique.

Useful results can also be obtained with anisotropic rocks, although independent information on the magnitude of the anisotropy and the orientation of the principal conductivity axes in situ is also required [5]. If porosity measurements are to be made on high-permeable rock fragments, control tests should also be made on similar solid-core samples to check the bulk volume determinations. No inconsistencies were noted in the results from the range of rocks tested in this study, but calculations suggest that, with the use of the vacuum in the bulk-volume measurements, mercury will enter the rock pores connected by channels greater than 0.006 mm diameter. In this case, trapped pockets of air may be removed by the use of a mechanical vibrator on the system, with or without the aid of a reduced vacuum, or by very loose packing of the chips and using a very slow rate of advance of the mercury into the chamber.

The development of the chip conductivity technique and its extension to porous rocks where no borehole-porosity information is available should allow terrestrial heat-flow measurements to be made in many existing boreholes which were previously unsuitable. It is hoped that this will enable geothermal data to be collected relatively inexpensively from

new areas, and make a valuable contribution to the understanding of the thermal mechanisms within the Earth.

## Acknowledgements

I would like to thank P. Threadgold for useful discussions in the early stages of this study, and G. Langley and P. Read for advice and assistance in making the porosity determinations. The British Petroleum Co. Ltd. allowed access to the Kobe porosimeter used in this study. Temperature measurements and sample collection in Cyprus were made with the kind permission and assistance of the Director and Staff of the Cyprus Geological Survey Department. Finally I would like to thank D.D. Blackwell and A. Richardson for their help and constructive criticism of the draft of this manuscript.

## References

- 1 F. Birch, Heat flow in the Front Range, Colorado, *Bull. Geol. Soc. Am.* 61 (1950) 567.
- 2 A.E. Beck, A steady state method for the rapid measurement of the thermal conductivity of rock, *J. Sci. Instrum.* 34 (1957) 186.
- 3 A.E. Beck, Techniques of measuring heat flow on land, In: W.H.K. Lee (Editor), *Terrestrial Heat Flow*, Geophys Monogr. Ser. No. 8 (1965) 24 pp.
- 4 A.M. Jessop, The effect of environment on divided bar measurements, *Tectonophysics* 10 (1970) 39.
- 5 J.H. Sass, A.H. Lachenbruch and R.J. Munroe, Thermal conductivity of rocks from measurements on fragments and its application to heat flow determinations, *J. Geophys. Res.* 76 (1971) 3391.
- 6 W. Woodside and J.H. Messmer, Thermal conductivity of porous media, *J. Appl. Phys.* 32 (1961) 1988.
- 7 C.M. Beeson, The Kobe porosimeter and the oilwell research porosimeter, *Am. Inst. Min. Metall. Pet. Eng., Trans.* 189 (1950) 313.
- 8 P. Morgan, *Terrestrial heat flow studies in Cyprus and Kenya*, Ph. D. Thesis, University of London (1973).
- 9 H.L. Ritter and L.C. Drake, Pore size distribution in porous materials, *Ind. Eng. Chem., Anal. Ed.* 17 (1945) 782.
- 10 K. Horai and G. Simmons, Thermal conductivity of rock-forming minerals, *Earth Planet. Sci. Lett.* 6 (1969) 359.
- 11 R. von Herzen and A.E. Maxwell, The measurement of thermal conductivity of deep-sea sediments by a needle-probe method, *J. Geophys. Res.* 64 (1959) 1557.
- 12 W. King and G. Simmons, Heat flow near Orlando, Florida



- and Uvalde, Texas determined from well cuttings, *Geothermics* 1 (1972) 133.
- 13 K. Horai, Thermal conductivity of rock-forming minerals, *J. Geophys. Res.* 76 (1971) 1278.
  - 14 E.C. Robertson and D.L. Peck, Thermal conductivity of vesicular basalt from Hawaii, *J. Geophys. Res.* 79 (1974) 4875.
  - 15 E.C. Bullard, Heat flow in South Africa, *Proc. R. Soc. London, Ser. A* 173 (1939) 474.
  - 16 E.C. Bullard, The disturbance of the temperature gradient in the Earth's crust by inequalities of height, *Mon. Not. R. Astron. Soc., Geophys. Suppl.* 4 (1940) 360.
  - 17 F.R.S. Henson, R.V. Browne and J. McGinty, A synopsis of the stratigraphy and geological history of Cyprus, *Q. J. Geol. Soc. London* 105 (1949) 1.
  - 18 E. de Vaumas, Further contributions to the geomorphology of Cyprus, In: *Annual Report for the Year 1960*, Geol. Surv. Dep., Nicosia, (1961) 24 pp.
  - 19 A.J. Erickson, The measurement and interpretation of heat flow in the Mediterranean and Black Sea, Ph.D. Thesis, Massachusetts Institute of Technology, Cambridge, Mass. (1970).
  - 20 W.B.F. Ryan, D.J. Stanley, J.B. Hersey, D.A. Fahlquist and T.D. Allan, The tectonics and geology of the Mediterranean Sea, In: A.E. Maxwell (Editor), *The sea*, 4 II, Wiley-Interscience, New York, N.Y. (1970) 387 pp.

I. In  
 T  
 ingto  
 as a s  
 orate  
 of a s  
 [1],  
 (Fo,  
 ene,  
 Alpin  
 is alm  
 margi  
 son [  
 the p  
 depth  
 that t  
 with a  
 eters  
 superi  
 acteri  
 grains  
 cleava  
 descri

